Force Correlations in Disordered Magnets

Cathelijne ter Burg,[1] Felipe Bohn,[2] Gianfranco Durin,[3] Rubem Luis Sommer,[4] and Kay Jörg Wiese[1]
[1]Laboratoire de Physique de l'École Normale Supérieure, ENS, Université PSL, CNRS, Sorbonne Université, Université Paris-Diderot, Sorbonne Paris Cité, 24 rue Lhomond, 75005 Paris, France
[2]Departamento de Física, Universidade Federal do Rio Grande do Norte, 59078-900 Natal, RN, Brazil
[3]Istituto Nazionale di Ricerca Metrologica, strada delle Cacce 91, 10135 Torino, Italy
[4]Centro Brasileiro de Pesquisas Físicas, Rua Dr. Xavier Sigaud 150, Urca, 22290-180 Rio de Janeiro, RJ, Brazil

(Received 17 December 2021; accepted 15 August 2022; published 2 September 2022)

We present a *proof of principle* for the validity of the functional renormalization group, by measuring the force correlations in Barkhausen-noise experiments. Our samples are soft ferromagnets in two distinct universality classes, differing in the range of spin interactions, and the effects of eddy currents. We show that the force correlations have a universal form predicted by the functional renormalization group, distinct for short-range and long-range elasticity, and mostly independent of eddy currents. In all cases correlations grow linearly at small distances, as in mean-field models, but in contrast to the latter are bounded at large distances. As a consequence, avalanches are anti-correlated. We derive bounds for these anticorrelations, which are saturated in the experiments, showing that the multiple domain walls in our samples effectively behave as a single wall.

DOI: 10.1103/PhysRevLett.129.107205

Each theory of disordered systems relies on specific assumptions, and often their validity is checked only for standard observables, such as the roughness exponent. Measuring its central ingredients would be a much more stringent test to discriminate between them. Two general theories have been proposed: the Gaussian variational ansatz invoking replica-symmetry breaking [1–3], which is exact for fully connected models [4,5], and the functional renormalization group (FRG) for short-ranged elastic systems [6,7], where the central ingredient is the effective force correlator. This correlator is the solution of a nonlinear partial differential equation [6–8], and can experimentally be extracted from the center-of-mass fluctuations of the interface.

To prove the validity of the FRG for disordered systems, we analyze the domain-wall motion in soft magnets (the Barkhausen noise) [9], the oldest example of depinning and avalanche motion [8,10–12]. Standard observables as the avalanche size, duration [13,14] and shape [15–18] show the existence of two universality classes differing in the kind and range of domain-wall interactions [12,14]: amorphous materials with short-range (SR) interactions and polycrystals with long-range (LR) interactions, consequence of strong dipolar effects. In 3D magnets, the latter is described by mean-field models pioneered in 1990 by Alessandro, Beatrice, Bertotti and Montorsi (ABBM) [19–21], where a domain wall is represented by a single degree of freedom, its center of mass (c.m.), a.k.a. *mean field* (MF). For the SR class, key observables as the avalanche-size exponent $\tau \simeq 1.27$ differ from their MF prediction $\tau_{\mathrm{MF}} = 3/2$, while they are accounted for by field-theoretic models [22–24].

In view of the solid evidence for exponents, a central question is whether experiments can contradict the ABBM model in a key prediction for LR magnets. We show that this is the case for the force correlator acting on the domain wall, or, equivalently, the correlator of its c.m. To understand this, consider the equation of motion of a d-dimensional interface with SR interactions,

$$\eta \partial_t u(x,t) = \nabla^2 u(x,t) + m^2[w - u(x,t)] + F(x, u(x,t)), \qquad w = vt. \tag{1}$$

Here w is proportional to the external applied field, increased very slowly, and m^2, usually denoted k, is the *demagnetization factor* [12]. Averaging Eq. (1) over x, given w, we get $\eta \dot{u}_w = m^2[w - u_w] + F_w$. Most of the time $\dot{u}_w = 0$, and the position and force correlations are

$$\hat{\Delta}_v(w - w') := \overline{[w - u_w][w' - u_{w'}]}^c \simeq \frac{1}{m^4} \overline{F_w F_{w'}}^c, \tag{2}$$

where the overbar designates a disorder average and ^{c} its connected part. In practice it is taken both over w and runs. $\hat{\Delta}_v$ depends on the driving velocity. Its zero-velocity limit,

$$\hat{\Delta}(w) = \lim_{v \to 0} \hat{\Delta}_v(w), \tag{3}$$

is the central object of the FRG field theory [7,8,25–27].

In an experiment, it is impossible to take $v \to 0$. The effect of $v > 0$ is to round the cusp $|\hat{\Delta}'(0^+)| = \sigma$ [see Eq. (6)] in a boundary layer of size $\delta_w \sim v\tau$, where

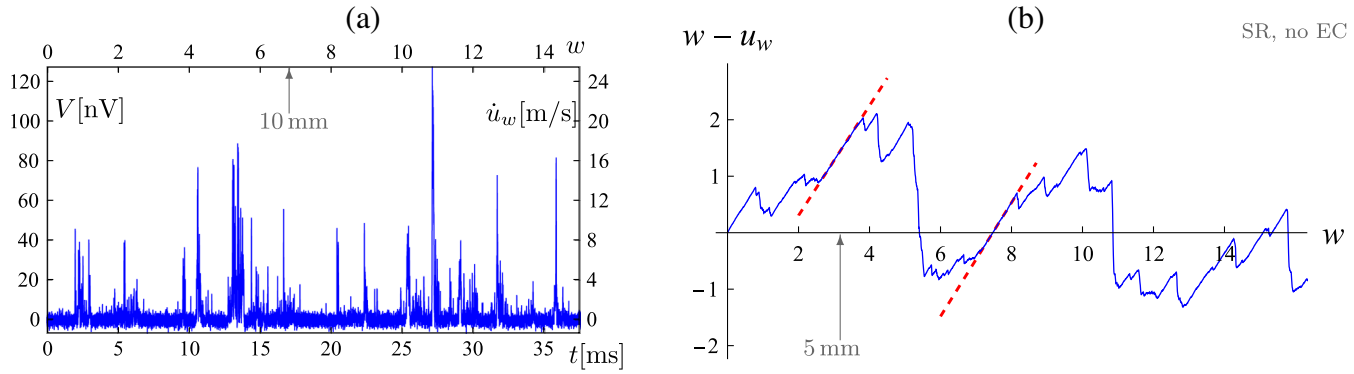

FIG. 1. Barkhausen noise in an amorphous FeSiB film (Table I). (a) Voltage signal recorded in the experiment (left axis), and corresponding domain-wall velocity $\dot{u}_w$ (right axis), as a function of time (bottom axis) and w (top axis). (b) The connected part of the interface position, $w - u_w$, obtained by integrating $\dot{u}_w$. $w = 1$ corresponds to 2.5 ms≈1.5 mm. Physical units are indicated by gray arrows.

τ is the timescale set by the response function $R(t) \simeq (1/\tau)e^{-t/\tau}$ [see Fig. 2(c) for an example]. Reference [28] shows that

$$\hat{\Delta}_v(w) = \int_0^\infty dt \int_0^\infty dt'\, R(t)R(t')\hat{\Delta}(w - v(t - t')) \qquad (4)$$

can be deconvoluted to reconstruct $\hat{\Delta}(w)$ from the measured $\hat{\Delta}_v(w)$ (see Supplemental Material [29], Appendix D). The result is

$$\hat{\Delta}(w) = \hat{\Delta}_v(w) + \tau^2 \hat{\Delta}_{\dot{u}}(w), \qquad (5)$$

where $\hat{\Delta}_{\dot{u}}(w)$ is the autocorrelation function of the measured $\dot{u}_w$. This allows us to extract $\hat{\Delta}(w)$ by plotting the rhs and finding τ that best eliminates the rounding close to $w = 0$. As shown below, Eq. (5) allows us to remove a boundary layer of size $\delta_w = v\tau$, but it creates a smaller one of size $\delta'_w = v\tau'$, see Supplemental Material [29], Appendix E.

The ABBM model assumes that forces F_w perform a random walk, and as a consequence

$$\frac{1}{m^4}\frac{1}{2}\overline{[F_w - F_{w'}]^2} = \hat{\Delta}(0) - \hat{\Delta}(w - w') \simeq \sigma|w - w'|. \qquad (6)$$

Field theory [8,30,31] predicts $\hat{\Delta}(0) - \hat{\Delta}(w)$ to grow linearly as Eq. (6) for small w, and to saturate for large w, with distinct shapes in SR and LR systems (see Supplemental Material [29], Appendix C). While this framework was tested in simulations [28,32], and experiments on wetting [33] and RNA/DNA peeling [34], only with magnets we can consider two universality classes, and with a large statistics.

We analyze our experimental data as follows. We start from the Barkhausen-noise time series, proportional to the c.m. velocity $\dot{u}_w$ [see Fig. 1(a)]. The signal is characterized by bursts when the domain wall moves forward, and a vanishing signal when it is pinned, i.e., at rest, combined with background noise (without noise $\dot{u}_w \geq 0$ [35]). This allows us to reconstruct the position of the c.m. u_w [see Eq. (2)], as depicted in Fig. 1(b). It is characterized by linearly increasing parts with slope 1, corresponding to an increasing magnetic field (i.e., w), followed by drops in $w - u_w$ when the wall moves forward. This allows us to reconstruct the unknown scale between $\dot{u}_w$ and the voltage induced in the pickup coil, reducing the scales in the experiment to a single one (see Supplemental Material [29], Appendix B).

We analyze $\hat{\Delta}(w)$ in different materials, summarized in Table I. We also consider data where eddy currents (EC) play a noticeable effect [9,12,15,16], an aspect experimentally tunable by varying the sample thickness [9,15,16]. Details on samples are given in Appendix A, and on the data analysis in Appendix F [29], including conversion of our units of w to physical space and time.

SR interactions without ECs. Our first sample is an amorphous 200-nm-thick FeSiB film. Figure 2(a) shows that the raw data for $\hat{\Delta}(w)$ are rounded in a boundary layer of size $\delta_w \approx 0.6$, due to the finite driving velocity. To obtain $\hat{\Delta}(w)$, we use Eq. (5) with $\tau = 0.17$. This reduces the boundary layer (nonstraight part) from $\delta_w \approx 0.6$ to $\delta_w \approx 0.1$, allowing us to extrapolate to $w = 0$ [gray in Figs. 2(a) and 2(b)]. The measured values for $\hat{\Delta}(0)$ and $\hat{\Delta}'(0^+)$ are then used to fix all scales in the theory predictions we wish to compare to on Fig. 2(b). These are

TABLE I. Short-range and long-range samples, with and without eddy currents.

Sample	Interactions/eddy currents	Correlation length ρ
Amorphous FeSiB film	SR/no	7.5 ms ≈ 495 μm
Amorphous FeCoB ribbon	SR/yes	0.1 s ≈ 67.5 μm
Polycrystalline NiFe film	LR/no	12.5 ms ≈ 500 μm
Polycrystalline FeSi ribbon	LR/yes	35 ms ≈ 0.9695 μm

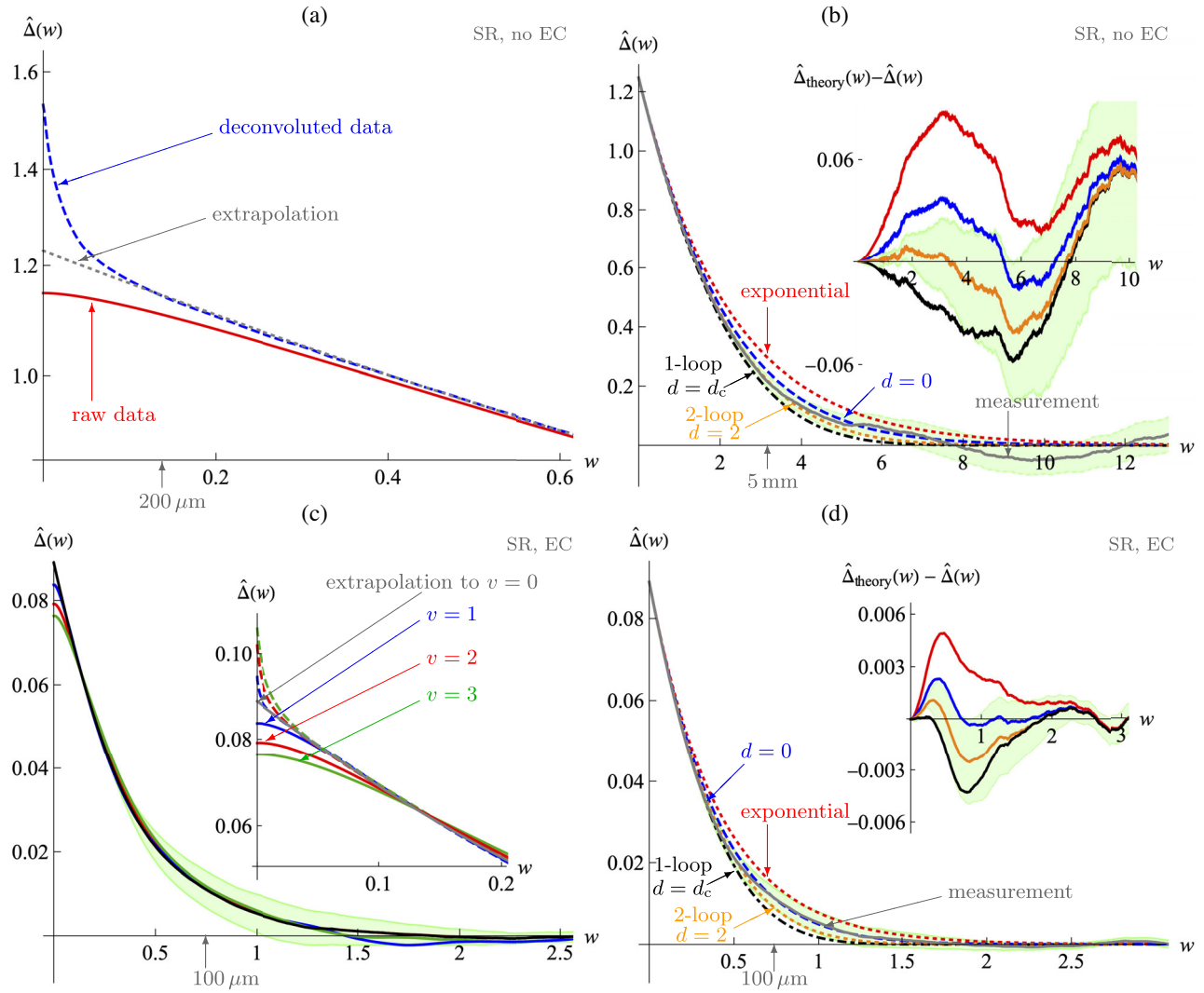

FIG. 2. (a) Construction of $\hat{\Delta}(w)$ for the FeSiB film (SR, no ECs). In red the raw data. In blue dashed, the result from Eq. (5) using $\tau = 0.17$. In dotted gray the extrapolation to $w = 0$. (b) Comparison of $\hat{\Delta}(w)$ using the dotted gray curve of (a), to theory candidates, fixing scales by $\hat{\Delta}(0)$ and $\hat{\Delta}'(0^+)$. The latter are from top to bottom: exponential (red, dotted), solution in $d = 0$ [28,36] (blue, dashed), 2-loop FRG via Padé for $d = 2$ (orange, dotted), 1-loop FRG (black, dot-dashed). Error bars in green for 1σ confidence intervals. The inset shows theory minus data in the same color code, favoring $d = 2$ FRG at two loops (with error bars for this curve only). (c) Check of deconvolution Eq. (5), for the FeCoB ribbon (SR, noticeable ECs), at different driving velocities v, using the same timescale $\tau = 0.025$; magnified in the inset. Apart from a small deviation for $v = 3$ they extrapolate to the same function. (d) Comparison of $\hat{\Delta}(w)$ from (c) to the theory, using the color code of (b). The data is consistent with 2-loop FRG in $d = 2$. $w = 1$ corresponds to 2.5 ms≈1.5 mm for (a)–(b), and to 0.2 s ≈ 135 μm for (c)–(d), see gray arrows.

from bottom to top (analytic expressions are in Appendix C. in the Supplemental Material [29]): 1-loop FRG (relevant for $d = d_c$, i.e., LR elasticity), 2-loop FRG in $d = 2$ (relevant for SR elasticity) [30,31], the $d = 0$ solution [28,36] and an exponential, the latter, not realized in magnets, given as reference. The data agree best, and within error bars, with the 2-loop FRG prediction for $d = 2$. From Fig. 2(b) we extract a correlation length $\rho := \hat{\Delta}(0)/\hat{\Delta}'(0) \approx 3$. This agrees with the scale on which $\hat{\Delta}_{\dot{u}}(w)$ decays to 0 [see Fig. 10(a) in Supplemental Material [29], Appendix G].

SR interactions with ECs. Our second sample with SR elasticity is an amorphous FeCoB ribbon where ECs are non-negligible. A range of different driving velocities is at our disposal. As ECs are more relevant as v increases, we focus on $v = 1$, 2, 3. There is additional (white) noise contributing to $\dot{u}$. After integration this contributes a linear function to $\hat{\Delta}(w)$, s.t.

$$\hat{\Delta}_v^{\text{raw}}(0) - \hat{\Delta}_v^{\text{raw}}(w) = \hat{\Delta}_v(0) - \hat{\Delta}_v(w) + \sigma_{\text{noise}}|w|, \quad (7)$$

necessitating to subtract a linear term $\sigma_{\text{noise}}|w|$ (see Fig. 8 in Supplemental Material [29], Appendix F2). Figure 2(c)

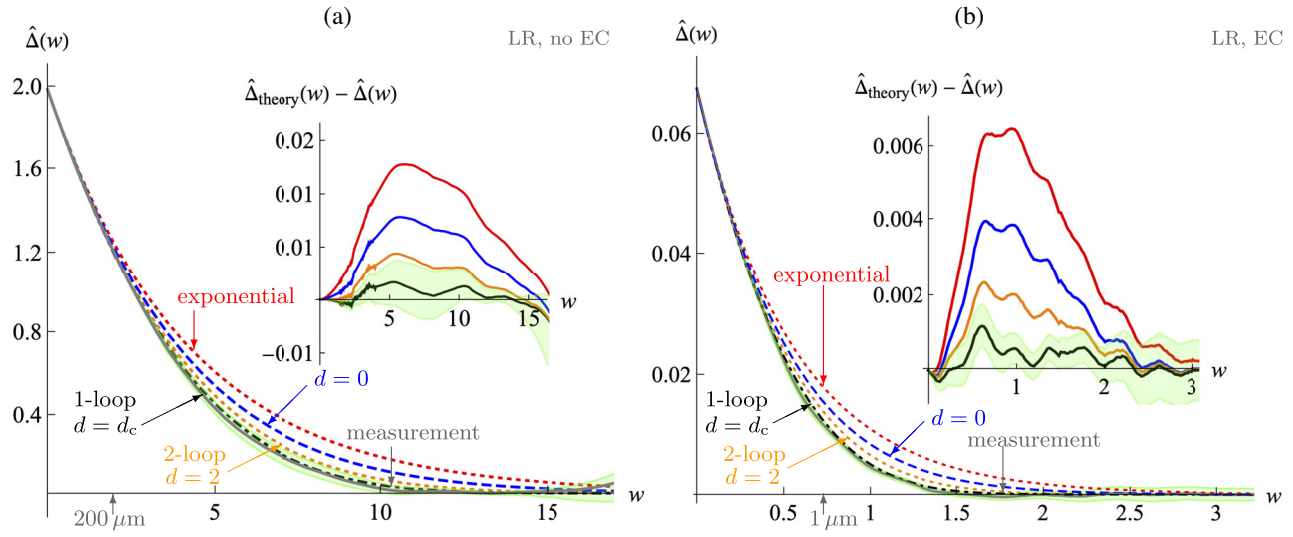

FIG. 3. The measured function $\hat{\Delta}(w)$ for our two LR samples: (a) a polycrystalline 200-nm-thick NiFe film (negligible ECs), and (b) a polycrystalline FeSi ribbon (with ECs). They agree with 1-loop FRG relevant here. $w = 1$ corresponds to 2.5 ms ≈ 100 μm for (a), and 50 ms ≈ 1.385 μm for (b), see gray arrows.

shows $\hat{\Delta}_v(w)$ after this subtraction. The inset zooms into the boundary layer with deconvolution by Eq. (5) in the same color code. Having data at different v allows us to test that (i) the boundary layer scales linearly in v, i.e., $\delta_w \sim v\tau$. (ii) $\hat{\Delta}_v(w)$ for $v = 1, 2, 3$ unfold to the same $\hat{\Delta}(w)$. Both conditions are satisfied using $\tau = 0.025$. Comparison to the theory proceeds as before, and is shown in Fig. 2(d), combining $v = 1$ and $v = 2$ to improve the statistics. Although error bars are non-negligible, the data is in agreement with the predicted 2-loop result in $d = 2$, as for FeSiB with SR elasticity without ECs in Fig. 2(b). For $w > 0.7$ the data slightly deviate from the 2-loop result, albeit well within error bars. Either this is a statistical fluctuation, or due to ECs.

LR interactions without ECs. LR elasticity arises in materials, here a polycrystalline 200-nm-thick NiFe film, due to strong dipolar interactions between parts of the domain wall. For long-range elasticity the upper critical dimension $d_c = 2$ coincides with the dimension of the wall. The common belief is that then MF theory, i.e., the ABBM model, is sufficient to describe the system. A glance at Fig. 3(a) shows that the experimental result is in contradiction to the prediction (6) of ABBM. While the latter holds at small w, at larger w the correlator $\hat{\Delta}(w)$ decays to zero. Field theory predicts [30,31,37,38] that fluctuations are relevant at the upper critical dimension, and that $\hat{\Delta}(w)$ is given by 1-loop FRG. Figure 3(a) shows that this is indeed the case.

LR interactions with ECs. Our fourth sample is a polycrystalline FeSi ribbon where the elasticity is LR and ECs are non-negligible. Figure 3(b) shows a comparison of $\hat{\Delta}(w)$ to the four theory candidates. As for the NiFe film with LR elasticity and no ECs, the agreement is excellent with 1-loop FRG, and inconsistent with ABBM. We refer to Supplemental Material [29], Appendix F4 and Fig. 9 for details on the data analysis for this sample.

In experiments, force correlations are bounded, and do not grow indefinitely as in MF models such as ABBM [19–21], see Eq. (6). As a consequence [Ref. [8] Sec. 4.20, or [39], Eq. (8)], avalanches are anticorrelated,

$$\frac{\langle S_{w_1} S_{w_2} \rangle}{\langle S \rangle^2} - 1 = -\hat{\Delta}''(w_1 - w_2). \tag{8}$$

Here S_w is the size of an avalanche at w, and $\langle S_w \rangle = \langle S \rangle$. The numerator $\langle S_{w_1} S_{w_2} \rangle$ is the expectation of the product of avalanche sizes, given that one is triggered at $w = w_1$, and a second at $w = w_2$; it depends on $|w_1 - w_2|$, and is averaged over the remaining variable. The experimental verification of this relation is shown on Fig. 4. Despite large statistical fluctuations, both the functional form as the amplitude agree. Since $\hat{\Delta}(w)$ is convex, $\hat{\Delta}''(w) \geq 0$. On the other hand, $\langle S_{w_1} S_{w_2} \rangle \geq 0$, thus $\hat{\Delta}''(w) \leq 1$. This bound is impossible to reach, as the toy-model [Supplemental Material [29], Eq. (C6)] in $d = 0$ has $\hat{\Delta}''(0^+) = 0.5$. The field theory [8] gives

$$\hat{\Delta}''(0^+) \leq \frac{2}{9} + 0.107\,533\varepsilon + \mathcal{O}(\varepsilon^2), \tag{9}$$

which evaluates to 0.437 for SR ($\varepsilon = 2$), and 0.222 ($\varepsilon = 0$) for LR correlations. Figure 4 shows that this bound is saturated, both for the SR and LR sample. This is surprising as both systems have multiple domain walls [40], estimated to be around five for the samples on Fig. 4. So either all but one domain wall are pinned, or these multiple walls are

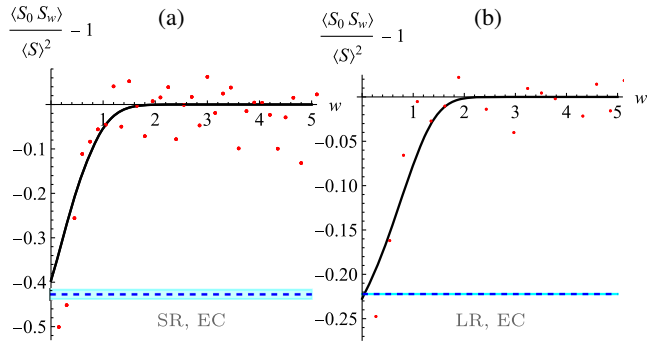

FIG. 4. Anticorrelation of avalanches as a function of w as defined in Eq. (8), for the two samples with ECs (red dots), (a) FeCoB with SR elasticity, and (b) FeSi with LR elasticity. The solid line is the prediction $-\hat{\Delta}''(w)$ of Eq. (8) from the experiment. The dashed lines are bounds on the maximal reduction from the field-theory (9), with error bars in cyan. $w = 1$ corresponds to 200 ms $\approx$ 135 μm for (a) and 50 ms $\approx$ 1.385 μm for (b).

so highly correlated that they effectively behave as a single wall.

In this Letter, we measured the effective force or c.m. correlations showing that they have a universal form, predicted by the FRG, both for SR and LR elasticity and mostly independent of ECs. We prove that FRG, an alternative to replica symmetry breaking, correctly models subtle details such as the dependence on dimension and the range of interactions. We hope this work inspires the experimental community to look beyond commonly studied observables and beyond MF. Further experimental systems to explore are sheered colloids or foams, DNA unzipping, and earthquakes.

We thank A. Douin, F. Lechenault, G. Mukerjee, and A. Rosso for discussions. F. B. and R. L. S. acknowledge financial support from CNPq and CAPES.

[1] M. Mézard, G. Parisi, and M. A. Virasoro, *Spin Glas Theory and Beyond* (World Scientific, Singapore, 1987), 10.1142/0271.
[2] G. Parisi, Infinite Number of Order Parameters for Spin-Glasses, Phys. Rev. Lett. **43**, 1754 (1979).
[3] G. Parisi, The order parameter for spin glasses: A function on the interval 0-1, J. Phys. A **13**, 1101 (1980).
[4] M. Talagrand, *Mean Field Models for Spin Glasses, Volume I: Basic Examples* (Springer Verlag, Berlin, Heidelberg, 2011), 10.1007/978-3-642-15202-3.
[5] M. Talagrand, *Mean Field Models for Spin Glasses, Volume II: Advanced Replica-Symmetry and Low Temperature* (Springer Verlag, Berlin, Heidelberg, 2011), 10.1007/978-3-642-22253-5.
[6] D. S. Fisher, Interface Fluctuations in Disordered Systems: $5-\varepsilon$ Expansion, Phys. Rev. Lett. **56**, 1964 (1986).
[7] T. Nattermann, S. Stepanow, L.-H. Tang, and H. Leschhorn, Dynamics of interface depinning in a disordered medium, J. Phys. II (France) **2**, 1483 (1992).
[8] K. J. Wiese, Theory and experiments for disordered elastic manifolds, depinning, avalanches, and sandpiles, Rep. Prog. Phys. **85**, 086502 (2022).
[9] F. Bohn, G. Durin, M. A. Correa, N. R. Machado, R. D. Della Pace, C. Chesman, and R. L. Sommer, Playing with universality classes of Barkhausen avalanches, Sci. Rep. **8**, 11294 (2018).
[10] H. Barkhausen, Zwei mit Hilfe der neuen Verstärker entdeckte Erscheinungen, Phys. Z. **20**, 401 (1919).
[11] J. P. Sethna, K. A. Dahmen, and C. R. Myers, Crackling noise, Nature (London) **410**, 242 (2001).
[12] G. Durin and S. Zapperi, The Barkhausen effect, *The Science of Hysteresis*, edited by G. Bertotti and I. Mayergoyz (Academic Press, Amsterdam, 2006), Vol. II, pp. 181–267, 10.1016/B978-012480874-4/50014-2.
[13] O. Perkovic, K. Dahmen, and J. P. Sethna, Avalanches, Barkhausen Noise, and Plain Old Criticality, Phys. Rev. Lett. **75**, 4528 (1995).
[14] G. Durin and S. Zapperi, Scaling Exponents for Barkhausen Avalanches in Polycrystalline and Amorphous Ferromagnets, Phys. Rev. Lett. **84**, 4705 (2000).
[15] S. Zapperi, C. Castellano, F. Colaiori, and G. Durin, Signature of effective mass in crackling-noise asymmetry, Nat. Phys. **1**, 46 (2005).
[16] S. Papanikolaou, F. Bohn, R. L. Sommer, G. Durin, S. Zapperi, and J. P. Sethna, Universality beyond power laws and the average avalanche shape, Nat. Phys. **7**, 316 (2011).
[17] L. Laurson, X. Illa, S. Santucci, K. T. Tallakstad, K. J. Måløy, and M. J. Alava, Evolution of the average avalanche shape with the universality class, Nat. Commun. **4**, 2927 (2013).
[18] G. Durin, F. Bohn, M. A. Correa, R. L. Sommer, P. Le Doussal, and K. J. Wiese, Quantitative Scaling of Magnetic Avalanches, Phys. Rev. Lett. **117**, 087201 (2016).
[19] B. Alessandro, C. Beatrice, G. Bertotti, and A. Montorsi, Domain-wall dynamics and Barkhausen effect in metallic ferromagnetic materials. I. Theory, J. Appl. Phys. **68**, 2901 (1990).
[20] B. Alessandro, C. Beatrice, G. Bertotti, and A. Montorsi, Domain-wall dynamics and Barkhausen effect in metallic ferromagnetic materials. II. Experiments, J. Appl. Phys. **68**, 2908 (1990).
[21] F. Colaiori, Exactly solvable model of avalanches dynamics for Barkhausen crackling noise, Adv. Phys. **57**, 287 (2008).
[22] D. S. Fisher, Collective transport in random media: From superconductors to earthquakes, Phys. Rep. **301**, 113 (1998).
[23] A. Dobrinevski, P. Le Doussal, and K. J. Wiese, Avalanche shape and exponents beyond mean-field theory, Europhys. Lett. **108**, 66002 (2014).
[24] A. Dobrinevski, Field theory of disordered systems—avalanches of an elastic interface in a random medium, Ph.D thesis, ENS Paris, 2013.
[25] P. Le Doussal and K. J. Wiese, How to measure Functional RG fixed-point functions for dynamics and at depinning, Europhys. Lett. **77**, 66001 (2007).

[26] O. Narayan and D. S. Fisher, Threshold critical dynamics of driven interfaces in random media, Phys. Rev. B **48**, 7030 (1993).
[27] P. Le Doussal, Finite temperature Functional RG, droplets and decaying Burgers turbulence, Europhys. Lett. **76**, 457 (2006).
[28] C. ter Burg and K. J. Wiese, Mean-field theories for depinning and their experimental signatures, Phys. Rev. E **103**, 052114 (2021).
[29] See Supplemental Material at http://link.aps.org/supplemental/10.1103/PhysRevLett.129.107205 for details on the samples, the data analysis, error estimates, and the field theory.
[30] P. Chauve, P. Le Doussal, and K. J. Wiese, Renormalization of Pinned Elastic Systems: How Does It Work Beyond One Loop?, Phys. Rev. Lett. **86**, 1785 (2001).
[31] P. Le Doussal, K. J. Wiese, and P. Chauve, 2-loop functional renormalization group analysis of the depinning transition, Phys. Rev. B **66**, 174201 (2002).
[32] A. Rosso, P. Le Doussal, and K. J. Wiese, Numerical calculation of the functional renormalization group fixed-point functions at the depinning transition, Phys. Rev. B **75**, 220201(R) (2007).
[33] P. Le Doussal, K. J. Wiese, S. Moulinet, and E. Rolley, Height fluctuations of a contact line: A direct measurement of the renormalized disorder correlator, Europhys. Lett. **87**, 56001 (2009).
[34] K. J. Wiese, M. Bercy, L. Melkonyan, and T. Bizebard, Universal force correlations in an RNA-DNA unzipping experiment, Phys. Rev. Research **2**, 043385 (2020).
[35] A. A. Middleton, Asymptotic Uniqueness of the Sliding State for Charge-Density Waves, Phys. Rev. Lett. **68**, 670 (1992).
[36] P. Le Doussal and K. J. Wiese, Driven particle in a random landscape: Disorder correlator, avalanche distribution and extreme value statistics of records, Phys. Rev. E **79**, 051105 (2009).
[37] A. A. Fedorenko and S. Stepanow, Depinning transition at the upper critical dimension, Phys. Rev. E **67**, 057104 (2003).
[38] P. Le Doussal and K. J. Wiese, Higher correlations, universal distributions and finite size scaling in the field theory of depinning, Phys. Rev. E **68**, 046118 (2003).
[39] T. Thiery, P. Le Doussal, and K. J. Wiese, Universal correlations between shocks in the ground state of elastic interfaces in disordered media, Phys. Rev. E **94**, 012110 (2016).
[40] E. F. Silva, M. A. Corrêa, R. D. Della Pace, C. C. Plá Cid, P. R. Kern, M. Carara, C. Chesman, O. Alves Santos, R. L. Rodríguez-Suárez, A. Azevedo, S. M. Rezende, and F. Bohn, Thickness dependence of the magnetic anisotropy and dynamic magnetic response of ferromagnetic NiFe films, J. Phys. D **50**, 185001 (2017).